EQUILIBRIUM SALTATION: MASS FLUXES, AERODYNAMIC ENTRAINMENT, AND DEPENDENCE ON GRAIN PROPERTIES

JUDITH J. J. DOORSCHOT* and MICHAEL LEHNING

Swiss Federal Institute for Snow and Avalanche Research, Flüelastrasse 11, 7260 Davos Dorf, Switzerland

Abstract. An examination is given of the way in which the saltation layer is affected by the characteristics of the particles. Special attention is given to the potential importance of aerodynamic entrainment during steady state saltation, a topic for which the discussion is still unresolved. A new numerical model for saltation in steady state is presented, which is focused on the computation of the horizontal mass flux. The numerical computations, combined with physical arguments, suggest that aerodynamic entrainment plays a more important role than generally assumed so far. A comparison of the model results is made with previous models, and with measurements of snow saltation that have been reported in the literature.

Keywords: Aerodynamic entrainment, Mass flux, Rebound, Saltation.

1. Introduction

The transport of granular materials by a turbulent airflow is a subject that has been studied intensively for various purposes. The way in which sand is eroded and deposited by the wind determines the formation of dunes. On the other hand, wind transport of snow in Alpine terrain has a significant influence on the avalanche situation. Furthermore, the way snow is redistributed by the wind has important consequences for Alpine hydrology and vegetation. Also snow drift around buildings or roads can cause practical difficulties, and it is highly recommended to consider this problem in the design of the infrastructure. For this type of practical application, it is of great interest that grain transport models are developed with the emphasis on the accurate determination of the mass flux.

The transport that takes place in a shallow layer close to the ground, by grains becoming entrained, and following ballistic trajectories and hopping over the surface, is called saltation. There are three ways in which particles can start saltation: aerodynamic entrainment, rebound, or ejection. Aerodynamic entrainment is the process by which particles, initially laying still on the ground, are picked up by the turbulent airflow. Rebounding particles are the particles that already are in saltation, hit the surface and bounce off again, thus starting a new trajectory in saltation. The third possibility, ejection, takes place when surface particles that initially lay still

* E-mail: Doorschot@slf.ch

are launched into saltation due to the impact of an other particle onto the surface; this process is sometimes also referred to as 'splash'.

Research on the topic of saltation started with the classic work of Bagnold (1941), followed by the steady state theory of Owen (1964). Since then research on sand saltation has concentrated on finding a description of the physical processes of aerodynamic entrainment, rebound, ejection and particle-wind feedback. Several detailed numerical models have been developed for simulating the saltation process, e.g., the first-order turbulence closure models of Anderson and Haff (1991) and McEwan and Willetts (1991), and the 1.5-order closure model of Shao and Li (1999). For snow saltation the most common approach has been to look for empirical or semi-empirical relations between wind speed and mass flux (e.g., Pomeroy and Gray, 1990). Recent snow research has however also been moving in the direction of physical models (e.g., Gauer, 1999; Naaim et al., 1998).

There are, however, several differences in grain characteristics between sand and snow that should be considered when the formulations that that have been defined for sand saltation are adopted for snow. Newly fallen snow particles have a dendritic rather than a spherical shape, and this will have an influence on the elastic properties, which are important in the rebound process. Furthermore, during the process of snow drift the grain properties will change. Surface grains with a dendritic shape tend to be broken by impacting grains, thus the grains become smaller and more elastic in time, and the bulk density increases.

Related to this is the question of the relative importance of aerodynamic entrainment compared to rebound and ejection during steady state saltation. The attention that several researchers have given to this problem has not resolved the discussion about this topic, since their answers are in conflict. A solution to this problem is however of great significance for the formulation of equilibrium saltation.

The question of the relative importance of aerodynamic entrainment, rebound and splash during steady state saltation is strongly connected with the concepts of fluid threshold and impact threshold, as discussed by Bagnold (1941). The fluid threshold, τ_{tf}, is defined as the minimum value of the fluid shear stress at the surface required for the initiation of grain movement over a passive surface. In other words, for aerodynamic entrainment to occur, the fluid shear stress at the surface must exceed the fluid threshold. With the impact threshold, τ_{ti}, Bagnold indicated the lowest possible fluid shear stress required for an already saltating system to remain moving. His measurements indicated that the value of the impact threshold was approximately 0.8 times the fluid threshold. He explained these observations with the argument that it requires less energy for an already moving grain to continue rebounding, than it does for a surface grain to be entrained by the airflow. This might, however, not be true for highly inelastic grains, such as fresh snow.

Following on Bagnold's concept, Owen (1964) proposed that for a system to continue saltating, the fluid shear stress at the surface had to stay at impact threshold, independently of the free wind speed. Since Bagnold's impact threshold

was lower than the fluid threshold, this would indicate that the fluid shear stress at the surface would be below the value required for the entrainment of surface grains. Therefore, the hypothesis of Owen combined with Bagnold's measurements suggests that aerodynamic entrainment may not occur during steady state saltation.

Recently, the use of different numerical models has led to a range of answers regarding this question. According to McEwan and Willetts's model aerodynamic entrainment may be possible at steady state. On the other hand, Anderson and Haff's model predicts that at steady state the surface friction velocity falls to slightly below the fluid threshold. Shao and Li (1999) claim the surface shear stress is forced to the fluid threshold through the equation for aerodynamic entrainment. In the computations, they observe however that the shear stress remains at a higher value, but explain this as a limitation due to the grid size. The same condition is used for the snow drift model of Naaim et al. (1998): At steady state they also assume that the shear stress at the surface is at fluid threshold.

In this paper, a conceptual solution to this problem is proposed. Resulting from this discussion, it is concluded that some significant simplifications may be justified in the calculations of saltating mass fluxes by existing models. A new model is constructed, and a comparison between our model results, other model results, and measurements reported in the literature is presented. Such a simplified model is of great importance for operational applications, such as, for example, the calculation of snow drift distribution patterns.

2. Theory

2.1. PARTICLE TRAJECTORIES IN SALTATION

Let us assume that a grain starts to move in saltation with some initial velocity, and consider the particle trajectory. An estimate of the forces on a grain saltating over a flat surface then indicates that particle motion is mainly governed by inertial forces, drag forces and gravity (e.g., Gauer, 1999). When turbulent fluctuations are neglected, the equations of motion for a particle in a horizontal cross-wind are given by:

$$\frac{\partial^2 x}{\partial t^2} = -0.75 \frac{\rho_a}{\rho_p} \frac{U_r}{d} C_d \left(\frac{\partial x}{\partial t} - U(z) \right) \tag{1a}$$

$$\frac{\partial^2 z}{\partial t^2} = -0.75 \frac{\rho_a}{\rho_p} \frac{U_r}{d} C_d \frac{\partial z}{\partial t} - g. \tag{1b}$$

Here ρ_a denotes the density of air (in kg m^{-3}), ρ_p the particle density, d the particle diameter, U_r the relative velocity between particles and airflow, $U(z)$ the horizontal wind velocity as a function of height, and g the acceleration due to

gravity. Furthermore, x and z are the position co-ordinates of the particle; the x-direction is aligned parallel to the surface in the direction of particle motion, and the z-direction is perpendicular to the surface. The drag coefficient C_d is a function of the particle Reynolds number. The neglect of turbulent wind fluctuations on the particle trajectories is discussed extensively in Hunt and Nalpanis (1985). When the influence of turbulent eddies becomes great enough to significantly change the trajectories, the particles are not saltating anymore and a transition to suspension occurs.

For given initial and wind field conditions a numerical solution describing particle trajectories can be found from the Equation (1). From these trajectories also information about the particle concentration profile with height can be found; the concentration in a certain small height interval is given by the average residence time of the particles in that height interval, and this is inversely proportional to their vertical velocity (Anderson and Hallet, 1986). For identical trajectories this leads to a sharp peak in the concentration at the maximum height of the trajectory, since the vertical velocity goes to zero at this point. From measurements in wind tunnels it is known however that the particle concentration decreases rapidly with height. This concentration profile is explained by a large range in initial particle velocities and ejection angles, as was shown by Willetts and Rice (1989). They found that the rebound angle for sand grains in saltation varies between zero and a certain maximum, with the lower angles occurring more frequently.

Because of the presence of particles in the air flow, the wind velocity profile and the turbulence characteristics of the flow are modified. The Reynolds shear stress, i.e., the vertical turbulent momentum transfer of the air flow is decreased, because part of the momentum is transferred to the saltating grains. A decrease of the Reynolds shear stress implies that also the wind velocity is decreased. The vertical momentum transfer that is carried by the particles is called the grain-borne shear stress, and is given at a certain height by the difference in horizontal momentum between upgoing and downgoing particles. In the following it will be assumed that the saltation layer is within the constant flux layer and that we have neutral conditions. In the absence of particles, the wind has a logarithmic profile as a function of height (Stull, 1988) for this situation. Conservation of momentum then states that at steady state the sum of the grain-borne shear stress and the fluid (or air-borne) shear stress is constant with height and equals the total fluid shear stress above the saltation layer.

2.2. GENERAL CALCULATION OF THE MASS FLUX

Numerical calculations of the particle trajectories, using the equations of motion (1), can be used for determining the mass flux. The rebound of a particle can be regarded as a slightly inelastic, frictional collision with the surface. In the model of Anderson and Haff (1991) this is modelled by a linear spring-damping system, and includes tangential frictional forces. Their simulation results, as well as the meas-

ured results from McEwan and Willetts (1991), show however an approximately linear relationship between impact speed and rebound speed. We therefore propose a simplified relation, where the relative energy loss is dependent of the particle properties:

$$v_e^2 = r v_i^2. \tag{2}$$

Here v_e and v_i are the ejection and impact speed, and $(1 - r)$ is the fraction of energy that is lost in the collision. In this manner the trajectories of a rebounding grain can be computed repeatedly, and it can be seen whether saltation height and length increase or decrease for a certain combination of input parameters.

For the rate of aerodynamic entrainment N_{ae} (in m^{-2}) the commonly used relation is (Anderson and Haff, 1991):

$$N_{ae} = \eta_{ae}(\tau_a(0) - \tau_{tf}), \tag{3}$$

where η_{ae} is a coefficient of dimension N^{-1}, $\tau_a(0)$ is the air-borne shear stress at the surface (Pa) and τ_{tf} is the threshold shear stress for aerodynamic entrainment (i.e., the fluid threshold).

Remembering that for steady state the sum of the air-borne and grain-borne shear stresses in the saltation layer equals the total fluid shear stress above the saltation layer, the mass flux can be computed. The grain-borne shear stress τ_g is defined as

$$\tau_g = N \frac{m(\overline{u}_i - \overline{u}_e)}{\overline{t}}. \tag{4}$$

Here N denotes the total number of particles in saltation (m^{-2}), m is the particle mass, $\overline{u}_i$ and $\overline{u}_e$ are the mean horizontal components of the impact and ejection velocity, and $\overline{t}$ is the mean time for a particle trajectory in saltation. If the grain cloud consists of both rebounding and aerodynamically entrained particles, the steady state balance of the shear stresses is given by:

$$\tau_a(0) + N_{ae} \frac{m(\overline{u}_{i,ae} - \overline{u}_{e,ae})}{\overline{t}_{ae}} + N_r \frac{m(\overline{u}_{i,r} - \overline{u}_{e,r})}{\overline{t}_r} = \tau_s. \tag{5}$$

Here $\overline{u}_i$ and $\overline{u}_e$ are the average horizontal components of the impact and ejection velocity respectively, and τ_s is the fluid shear stress above the saltation layer. The subscripts ae and r denote aerodynamic entrainment and rebound, respectively. The particle velocities and trajectory duration can be deduced from Equation (1). Thus, Equation (5) can be solved for the mass flux when the shear stress at the surface is known, as will be discussed extensively in Section 2.4. The mass flux Q (kg m^{-1} s^{-1}) is given by

$$Q = N_{ae} m \overline{u}_{ae} + N_r m \overline{u}_r, \tag{6}$$

where $\overline{u}_{ae}$ is the average horizontal component of the velocity of an aerodynamic-ally entrained particle, and $\overline{u}_r$ is the average horizontal component of the velocity of a rebounding particle.

2.3. WIND PROFILE, AERODYNAMIC ENTRAINMENT RATE AND INITIAL CONDITIONS

For an analytic approximation of the wind profile in a saltation layer several expres-sions can be found in the literature. These formulations are based on analytic fits to either simulated or measured profiles, or in some cases are simply expressions that fit all logical conditions (McEwan, 1993).

The fluid shear stress profile in the saltation layer is reduced compared to the situation without saltation, due to the momentum transfer of the airflow to the particles. The profile has to obey the condition of approaching the total fluid shear stress at the height of the saltation layer. Above the saltation layer, the fluid shear stress stays at this value. Furthermore, both Anderson and Haff (1991) and Raupach (1991) state that the fluid shear stress should rise monotonically with height.

An analytical expression for the fluid shear-stress profile with height $\tau_a(z)$ proposed by Raupach (1991) fitting all the formulated conditions is

$$\tau_a(z) = \tau_s \left(1 - (1 - \sqrt{\tau_a(0)/\tau_s})\, e^{-z/h_s} \right)^2, \qquad (7)$$

in which τ_s represents the total fluid shear stress above the saltation layer, $\tau_a(0)$ is the shear stress at the surface, and h_s is the height of the saltation layer. We will make use of this expression, because we are interested in constructing a simple model of saltation for operational use. For an analysis of explicit feedback effects of particles on an atmospheric flow we refer to Bintanja (2000).

An important factor for the model outcome of the mass flux is the rate of aerody-namic entrainment under given wind conditions. In Equation (3) the aerodynamic entrainment rate is proportional to the coefficient η_{ae}. The value of this coefficient is however difficult to estimate, since literature values are only available for sand, and may vary by several orders of magnitude. For snow particles, we propose that the aerodynamic entrainment rate is proportional to the number of grains per unit area on the surface. This results in

$$\eta_{ae} = \frac{C_{ae}}{8\pi d^2}, \qquad (8)$$

where the parameter C_{ae} may be dependent on grain properties, such as grain shape and density. The exact nature of this dependency would need further investigation, and for the present simulations, the value of C_{ae} is set to 1.

For the initial conditions of the particle trajectory (velocity and ejection angle), the measurements of Nishimura and Hunt (2000) will be used for snow and ice particles.

2.4. FLUID SHEAR STRESS AT THE SURFACE

A key problem for the determination of the mass flux lies in the interaction between the fluid shear stress and the mass flux. The fluid shear stress profile, which may be given by Equation (7), is reduced due to the presence of the particles. This adaptation is governed in this equation by the parameter $\tau_a(0)$, the fluid shear stress at the surface. According to Equation (5) however, $\tau_a(0)$ is inversely related to the saltation mass. Thus, for determining the fluid shear-stress profile the mass flux needs to be known, and vice versa. This circular problem needs to be solved to calculate the mass flux with a fixed wind profile.

Let us consider the conditions for steady state, and the implied consequences for the saltation process. Due to the mutual feedback between fluid shear stress and mass flux, the saltation mass flux fluctuates around an equilibrium value. The direct consequence of that (Owen, 1964) is that the fluid shear stress at the surface falls to a value just sufficient to ensure the mobility of the surface grains. This leaves the question open as to how this mobility is established. In principle there are three options: aerodynamic entrainment, rebound of saltating grains, or ejection of new grains from the surface by the impact of another grain. In the following we will investigate which of these processes occurs for a certain particle under certain initial conditions, and calculate the mass flux based on this analysis.

The overall condition that must be satisfied for a saltating system in equilibrium, is that the mean replacement capacity, i.e., the average number of particles entering saltation after a collision with the surface, is smaller than one. What happens exactly after a certain collision, is dependent on the exact location where the saltating particle hits a surface particle. Thus, due to the roughness of the surface, the result of a grain collision with the ground is highly coincidental. This is reflected in the great scatter that has been measured in the initial velocity and angle of saltating grains (e.g., Nishimura and Hunt, 2000). In these measurements it is not specified whether grains are rebounding or ejected, and their presented trajectory parameters, which we use in our simulations, are an average resulting from different processes. Therefore, there is for our purpose on average no difference between a grain that rebounds and a grain that ejects a new grain from the surface. In the following analysis no distinction is made between rebound and ejection, and it is assumed that ejection can be modelled in the same manner as rebound. This includes the case when an individual impacting grain might eject more than one particle.

Let us start with the assumption that aerodynamic entrainment occurs exclusively, and rebound or ejection is not possible. Furthermore, it is assumed that all grains have the same size and enter saltation with the same initial conditions. For the rate of aerodynamic entrainment N_{ae} the commonly used relation is given by Equation (3). The particle trajectory can be calculated when the initial conditions are known. Furthermore, Equation (5) reduces to

$$\tau_a(0) + N_{ae}\frac{m(\overline{u}_{i,ae} - \overline{u}_{e,ae})}{\overline{t}_{ae}} = \tau_s.\tag{9}$$

Equations (3) and (9) contain two unknowns (N_{ae} and $\tau_a(0)$), and can principally be solved. The particle velocities and the hop time in (2.10) are dependent on the fluid shear stress at the surface, therefore the solution for N_{ae} and $\tau_a(0)$ needs to be computed iteratively. Thus, the fluid shear stress at the surface $\tau_a(0)$ can be calculated as a function of the overall fluid shear stress when it is assumed that saltation is governed by aerodynamic entrainment only. We will call this value of the surface shear stress the aerodynamic entrainment threshold τ_{ae}.

As a second case let us now assume that rebound is dominating, and aerodynamic entrainment does not occur. In this case Equation (5) reduces to

$$\tau_a(0) + N_r \frac{m(\overline{u}_{i,r} - \overline{u}_{e,r})}{\overline{t}_r} = \tau_s. \tag{10}$$

The same procedure is now applied to the rebound process, based on the concepts of weak and strong saltation, as was distinguished in the numerical simulations by Shao and Li (1999). For grains that enter the weak saltation regime the hop length and height decrease until a steady state is reached; in the strong saltation regime however the hop length and height keep increasing until steady state. In weak saltation the saltation height does not usually exceed the grain size, and therefore grains in weak saltation do not make a significant contribution to the mass flux. For this reason we assume that in nature the weak saltation mode does not exist, and rebounding grains must be in the strong saltation regime. Assuming that all trajectory parameters and grain properties do not change during the collision with the surface, the limit between weak and strong saltation is determined by the fluid shear stress at the surface. We will call this the rebound threshold τ_r, and it represents the condition at which a grain that starts moving stays at constant saltation height.

It should be noted that τ_{ae} is not the same as the fluid threshold τ_{tf}. Whereas τ_{tf} is the lowest value of the fluid shear stress at which aerodynamic entrainment can take place, τ_{ae} is the value of the fluid shear stress at the surface, at which saltation can be in equilibrium with aerodynamic entrainment only. Also, note that the rebound threshold τ_r is, by this definition, not identical to the impact threshold τ_{ti} as defined by Bagnold. Whereas the impact threshold is the lowest free stream fluid shear stress at which saltation is maintained (due to rebound), the rebound threshold is the lowest possible fluid shear stress at the surface (for a given value of the free stream fluid shear stress) at which rebound is possible.

We will now return to Owen's theory, which states that the fluid shear stress at the surface is at the lowest value for which the surface particles are still mobile. As a consequence, it can be concluded that the shear stress at the surface has to stay at either τ_r or τ_{ae}, whichever of these two is the lowest. When the surface shear stress is at rebound threshold τ_r, rebound is the dominant process, and the mass flux is obtained from Equation (10), which then contains only one unknown. When the fluid shear stress at the surface is at aerodynamic entrainment threshold, τ_{ae},

the dominant process is aerodynamic entrainment, and the mass flux is determined from Equations (3) and (6).

The assumption that is made so far of identical grains and identical trajectories is naturally unrealistic. The previous analysis may, however, also be interpreted as valid for one grain of given size and given initial conditions for its trajectory. Then, a range of particle sizes, initial ejection velocities, and initial ejection angles can be implemented, and the procedure of determining the dominant process can be repeated for every possible case. By including probability functions for particle size and initial conditions of the trajectory, the saltation process can be investigated with more realistic conditions.

3. Numerical Model of Steady State Saltation

3.1. MASS FLUX MODEL

From the previously described concept a numerical model was developed for calculating mass fluxes in steady state saltation. Although the steady state condition has the limitation that no studies can be made about the way in which this steady state is reached, it has the advantage that several gross simplifications can be made.

The particle trajectories are computed by a forward time-integration of the equations of motion (1). For the feedback between air flow and particle motion in these equations the wind profile is needed; this is constructed from the shear stress profile (7). The shear stress at the surface $\tau_a(0)$ needs to be provided as the lower boundary condition, the free stream fluid shear stress τ_s as the upper boundary condition.

In order to know the lower boundary condition $\tau_a(0)$, the rebound threshold τ_r, and the aerodynamic entrainment threshold τ_{ae}, as defined in the previous section, are calculated. For determining the rebound threshold, a number of successive particle trajectories are calculated for a fixed value of the surface shear stress and free stream shear stress, to determine whether the process is in weak or in strong saltation. The surface shear stress is then iteratively adjusted, to find the rebound threshold. The aerodynamic entrainment threshold is determined by iteratively solving Equations (9) and (7).

Next, the surface shear stress is determined by the following rules:

if $(\tau_r > \tau_s) \Rightarrow \tau_a(0) = \tau_{ae}$ (aerodynamic entrainment only),

else, if $(\tau_{ae} < \tau_r) \Rightarrow \tau_a(0) = \tau_{ae}$ (aerodynamic entrainment only), and if $(\tau_{ae} > \tau_r) \Rightarrow \tau_a(0) = \tau_r$ (rebound only).

Thus, the shear stress at the surface is known and the wind profile is constructed from Equation (7), which allows for the computation of the particle trajectory. From there the average grain-borne shear stress (4) caused by one grain is known. The total number of saltating grains is calculated from Equation (9) or (10), and

the mass flux from Equation (6). The resulting mass flux is integrated over height, i.e., in units of (kg m^{-1} s^{-1}). The roughness height is parameterised as a function of grain size:

$$z_0 = d/10. \tag{11}$$

The ejection velocity and the ejection angle, as well as the grain size, are kept constant, and their input values for the simulations are taken from the measurements of Nishimura and Hunt (2000). The ejection velocity is assumed to be proportional to the friction velocity.

3.2. STOCHASTIC MODEL

A modified version of the model was developed for examining how realistic the assumption is of a saltating cloud existing of either rebounding or entrained grains exclusively. In this version, a range of initial conditions and particle sizes is implemented.

The measurements of Nalpanis et al. (1993), Nishimura et al. (1998) and Nishimura and Hunt (2000) demonstrate that it is plausible that the range of the ejection velocity and ejection angle, as well as the particle size, are well represented by a log-normal distribution. The correlation between ejection angle and ejection velocity measured by Nishimura and Hunt (2000) is very low, therefore these parameters are independent in our simulations.

The numerical procedure of the idealised model is then repeated for all combinations of ejection velocity, ejection angle and grain diameter. In this way a system is constructed in which aerodynamic entrainment and rebound exist simultaneously.

4. Results

4.1. TRAJECTORY AND MASS FLUX COMPUTATIONS

In Figure 1 an example is presented of computations of particle trajectories (a), particle velocity (b) and acceleration (c) as a function of height. In the plot of the particle velocity (b) the wind velocity is also shown. The arrows in Figures 1b and 1c indicate the direction of progressing time. An interesting point to note from this diagram is the fact that close to the ground the particle velocity is greater than the wind velocity, for both upgoing and downgoing particles. This must principally happen, regardless of what the wind profile looks like, since the wind velocity at the surface goes to zero and the particle velocity does not.

Figure 2 presents the surface shear velocity at rebound threshold τ_r and aerodynamic entrainment threshold τ_{ae}, as defined in Section 2.4, as a function of the free stream shear velocity. The shear (or friction) velocity is defined by $u_* = (\tau_s/\rho_a)^{0.5}$. The solid lines represent the rebound threshold for different values of the rebound
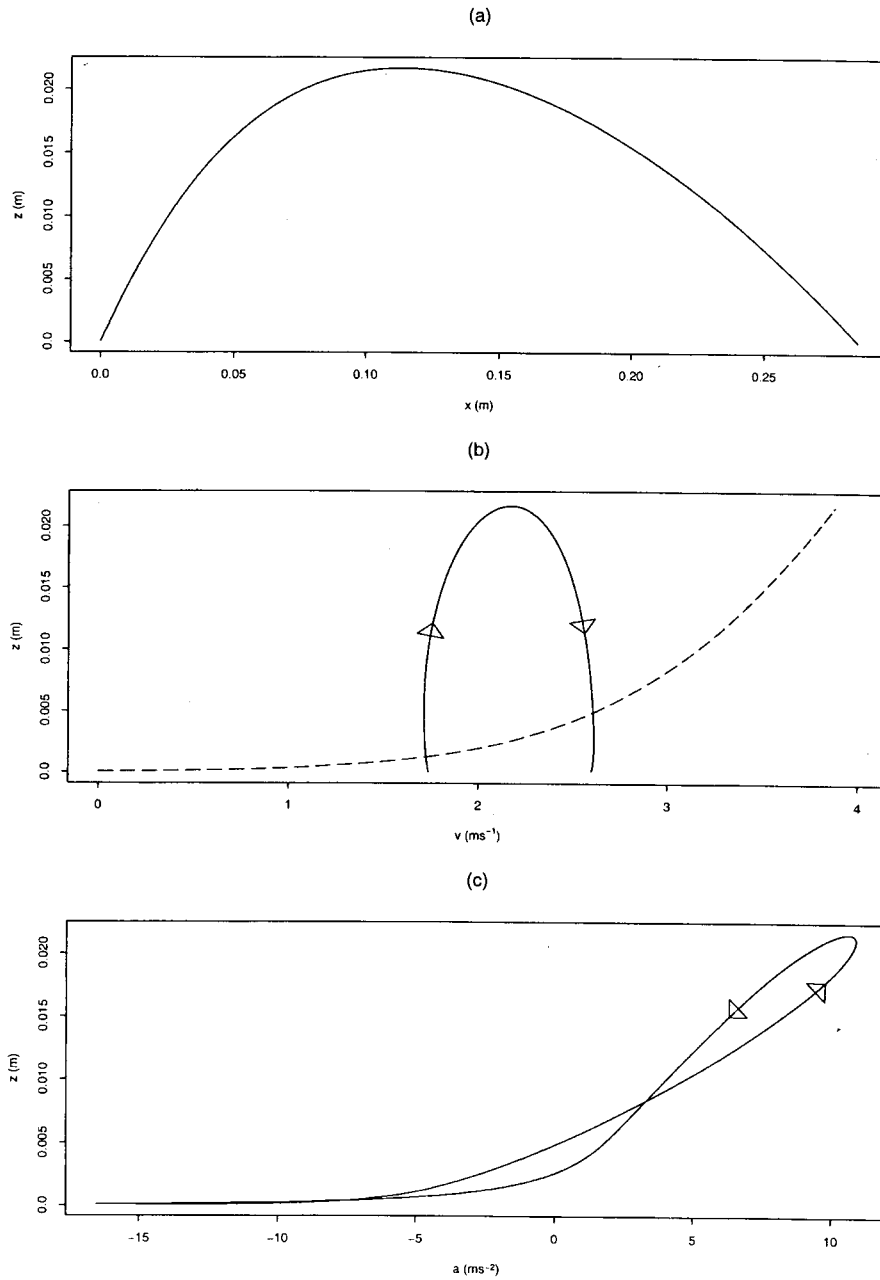
(a)

(b)

(c)

Figure 1. Results of computations: Particle trajectory (a), velocity (b) and acceleration (c). In figure (b) the solid line indicates the particle velocity and the dashed line indicates the wind velocity. Model parameter values: $d = 0.00048$ mm, $v_{ej} = 1.74$ m s^{-1}, $\alpha_{ej} = 25°$. The arrows in (b) and (c) indicate the direction of progressing time.
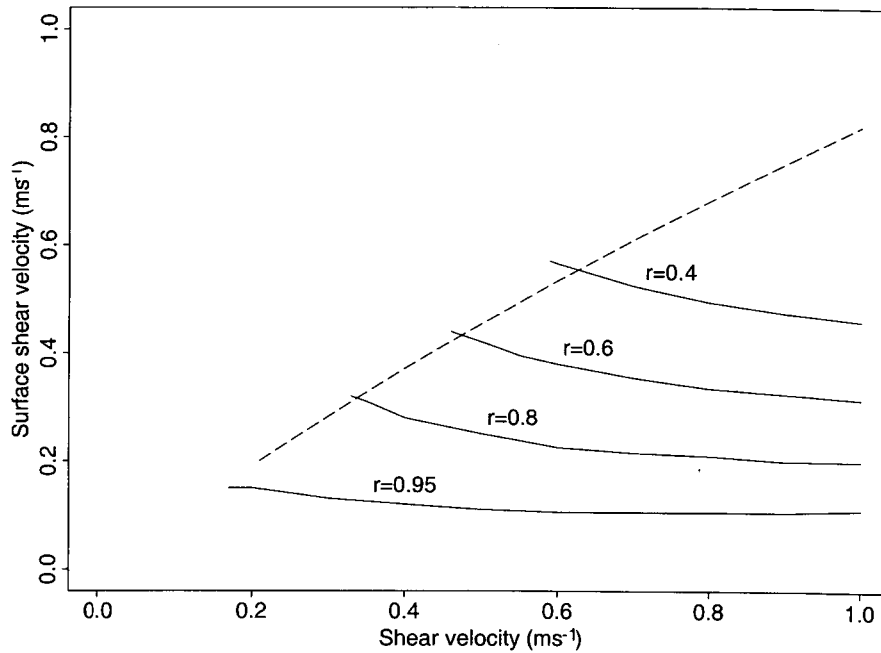
Figure 2. The relation between shear velocity and surface shear velocity at rebound threshold, for several values of the rebound parameter r. The dashed line indicates the aerodynamic entrainment threshold. The fluid threshold τ_{tf} is set to 0.2 m s^{-1}.

parameter r; the dashed line indicates the aerodynamic entrainment threshold. In the presented simulations the rebound angle has been kept constant at 30 degrees, the grain size at 1 mm and the threshold friction velocity at 0.2 m s^{-1}. It is seen that the rebound threshold increases with a decrease in the rebound parameter r. Furthermore, Figure 2 shows that for e.g., $r = 0.4$, the curve of the rebound threshold starts at a free stream friction velocity of about 0.55 m s^{-1}. This implies that at friction velocities lower than this value, rebound is not possible, and therefore aerodynamic entrainment must be the dominant process. The rebound threshold slowly decreases with an increase in free stream friction velocity, and approaches a constant value for large friction velocities.

From Figure 2 the relation between the rebound threshold τ_r, the impact threshold τ_{ti}, the aerodynamic entrainment threshold τ_{ae} and the fluid threshold τ_{tf} can be deduced. In this diagram, the impact threshold is the lowest value of the shear velocity for which the curve of the rebound threshold exists. It is seen that for $r = 0.95$ the impact threshold is about 0.18 m s^{-1}, which is lower than the fluid threshold of 0.2 m s^{-1}. This confirms, in a numerical way, the effect experimentally observed by Bagnold (1941), that an already existing saltation layer can be maintained at the shear velocity values below the fluid threshold. It may however also be concluded that this can only occur for particles with very high
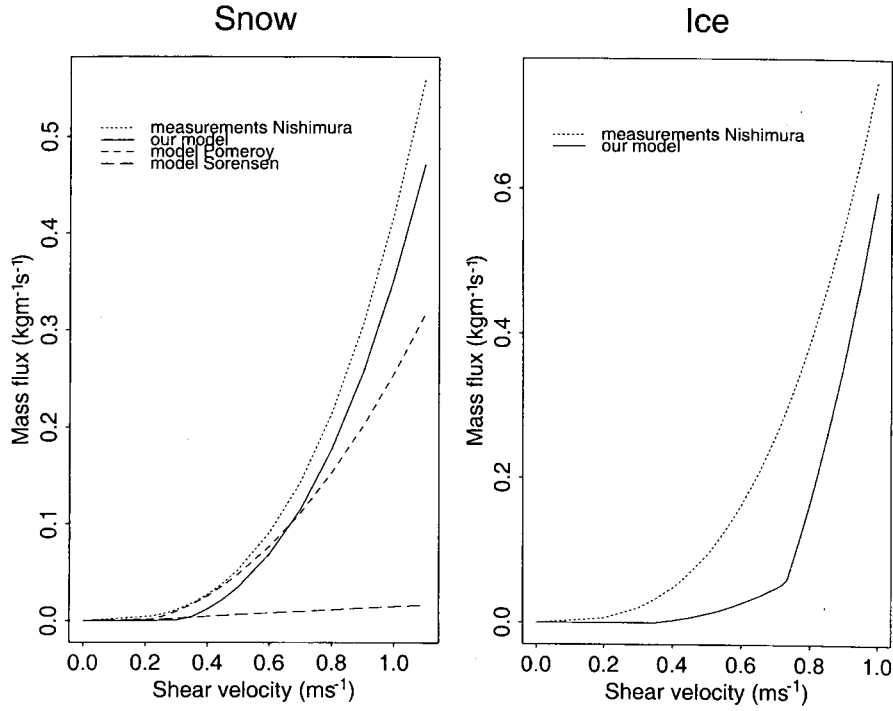
Snow

Ice

Figure 3. Comparison of mass flux computations and measurements (Nishimura and Hunt, 2000) for snow and ice particles, as a function of the friction velocity Model parameter values: snow d = 0.00048 m, r = 0.35, α_{ej} = 25°; ice d = 0.0028 m, r = 0.59, α_{ej} = 21°. In the diagram for the snow simulations, comparisons are also plotted with model results from Pomeroy and Gray (1990) and Sorensen (1991).

elasticity. For the aerodynamic entrainment threshold, it is seen that the surface friction velocity is only slightly smaller than the free stream friction velocity. The aerodynamic entrainment threshold is always greater than the fluid threshold.

For a comparison of our computed mass fluxes with measured values we use the wind-tunnel experiments of Nishimura and Hunt (2000), where values are found of saltation trajectory statistics for several particle types, and the associated mass flux. In Figure 3 a comparison between their measured and our computed mass fluxes is presented, as well as a comparison with two other saltation models. The first model that is used for comparison is from Sørensen (1991):

$$Q = 0.0014\rho_a u_*(u_* - u_{*th})(u_* + 7.6u_{*th} + 205),\tag{12}$$

where u_* is the free stream shear velocity and u_{*th} is the fluid threshold friction velocity, defined by $u_{*th} = (\tau_{tf}/\rho_a)^{0.5}$. The second model is from Pomeroy and Gray (1990):

$$Q = 0.68\frac{\rho_a u_{*th}}{gu_*}(u_*^2 - u_{*th}^2).\tag{13}$$

It is seen that our model produces a very good agreement with the snow measurements (d = 0.48 mm, u_{*th} = 0.20 m s^{-1}). Both other models show a larger underestimation of the mass fluxes, especially at higher shear velocities. For the ice particles (d = 2.80 mm, u_{*th} = 0.35 m s^{-1}) the computations show a underestimation of the mass flux of about 10 to 20 per cent. For these computations the ratio of impact to ejection velocity v_i/v_e = 1.3 has been used, as was measured for u_* = 0.5 m s^{-1}.

A point that is observed in the ice simulations is the clear transition between the dominant mechanisms for saltation. For friction velocities smaller than 0.75 m s^{-1} aerodynamic entrainment is responsible for the particle transport, and the mass flux increases rather slowly with increasing friction velocity. At friction velocities greater than 0.75 m s^{-1} the dominant mechanism is rebound, which causes a sharp increase in mass flux.

The sensitivity of the trajectories and the mass flux to a variation of the rebound parameter r is shown in Figure 4. In Figures 4a–c the saltation height h, saltation length l, and mass flux Q, respectively, are plotted as a function of r, for two different shear velocities. It is seen that the saltation height is not very sensitive to a variation in r. This is caused by the fact that the saltation height is mainly governed by the ejection velocity, which is only dependent on the shear velocity in our simulations. The saltation length however clearly decreases with an increase in r, the reason being that, with a low rebound parameter r, the fluid shear stress at the surface, and thus the wind velocity, is higher. Therefore the horizontal drag is greater, and a particle is transported over a greater distance before impact with the ground. The mass flux shows an exponential increase with an increase in r. In all three diagrams the transition between aerodynamic entrainment and rebound is seen for the simulations with a shear velocity of 0.3 m s^{-1}. For values of r that are smaller than 0.55 aerodynamic entrainment is the dominant process, which implies that r has no influence on the saltation length or height, or the mass flux.

A topic for which the discussion is not yet resolved, is the question of what the criterion is for the feedback of the particles on the wind to start to become important. As a contribution to this discussion, the relation between the air-borne shear stress and the grain-borne shear stress at the surface, as a function of the total fluid shear stress above the saltation layer, is presented in Figure 5. For these simulations, the same parameters were used as for the snow simulations shown in Figure 3. It is seen that for a low total shear stress the air-borne shear stress is much larger than the grain-borne shear, and thus the feedback of particles on the wind is small. For total fluid shear stress values greater than about 0.1 Pa, however, the grain-borne shear stress increases and becomes greater than the air-borne shear stress. After this transition the air borne shear stress remains approximately constant with an increase in total fluid shear stress. The transition between these phases occurs at the point where rebound becomes energetically more effective than aerodynamic entrainment. Thus, from these simulations it may be concluded that the feedback
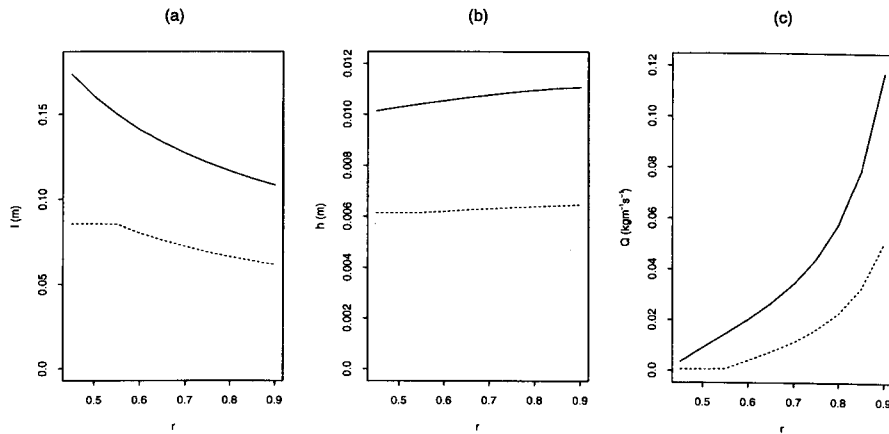
Figure 4. Saltation height (a), saltation length (b) and mass flux (c) as a function of r. The shear velocity is 0.3 m s^{-1} for the dashed line, and 0.4 m s^{-1} for the solid line. The grain size $d = 0.0048$ m.

of the saltating particles on the wind, and thus the modification of the wind profile, starts to play an important role when rebound is the dominant process in saltation.

4.2. STOCHASTIC MODEL: AERODYNAMIC ENTRAINMENT VERSUS REBOUND

The mass flux model used for the simulations has the advantage that some significant simplifications have been made compared to previous numerical models, while it still produces reliable results. For checking the validity of these simplifications, the advanced model described in Section 3.2 was used.

Figure 6 shows the ratio between aerodynamic entrainment and rebound for the snow simulations as presented in the previous section ($d = 0.48$ mm, $r = 0.35$, $\alpha_{ej} = 25°$). This may be important because of the influence of the transport mechanism on the mass flux, as was e.g., seen in Figure 3. In Figure 6 the percentage of particles in aerodynamic entrainment/rebound is plotted against the friction velocity. The solid lines show the simulations with the stochastic model (entrainment and rebound exist simultaneously); the dotted lines represent the simulations with the simplified model (the saltating cloud exists of entrained or rebounding grains exclusively).

It is clearly seen that at low friction velocity aerodynamic entrainment dominates, whereas at high friction velocity rebound is more important. This is seen both in the non-stochastic and the stochastic simulations. The friction velocity at which rebound starts to become more important is slightly lower for the non-stochastic simulations. It may be concluded that for low and high shear velocity the simplified approach is justified. For intermediate shear velocities the saltation layer, however, consists of a mixture of aerodynamically entrained and rebounding grains, and so explains the sharp transition observed in the mass flux for ice particles in Figure 3.

Another interesting point is observed in Figure 7a, which presents the ratio between aerodynamic entrainment and rebound as a function of the particle dia-
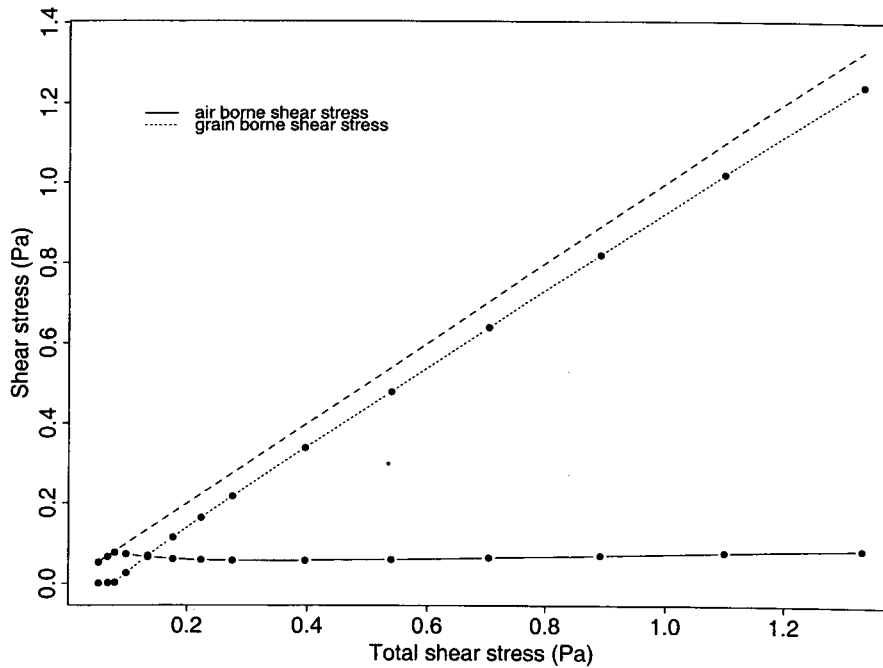
Figure 5. Grain-borne shear stress (dotted line) and air-borne shear stress (solid line) as a function of the total fluid shear stress above the saltation layer. The dashed line indicates the sum of the air-borne and the grain-borne shear stress. Model parameter values: $d = 0.00048$ m, $r = 0.35$, $\alpha_{ej} = 25°$.

meter ($u_* = 0.8$ m s^{-1}). All further parameters are the same as in the previously presented simulations for ice particles ($d = 2.8$ mm, $r = 0.59$, $\alpha_{ej} = 21°$). This figure indicates that aerodynamic entrainment may become more important for larger particles. Furthermore, Figure 7b shows that, related to this, the mass flux decreases for larger particles. Although these results may be surprising at first sight, they can however be well explained by returning to the equations of motion (1). In these equations the drag terms are inversely proportional to the grain size d. Thus, a large particle experiences a smaller drag force, and will be accelerated less than a small particle. Rebound can only occur when the total acceleration of the particle over the whole trajectory is large enough to counteract the loss of momentum during the collision with the surface. Therefore, large particles require higher wind speeds for maintaining rebound than do small particles.

5. Discussion and Conclusions

In this paper we presented a new numerical model aimed at the computation of mass fluxes in saltation, based on the assumption that the system is in equilibrium. This emphasis on the resulting mass flux is important for many practical applications, for example for calculating deposition patterns caused by blowing sand or
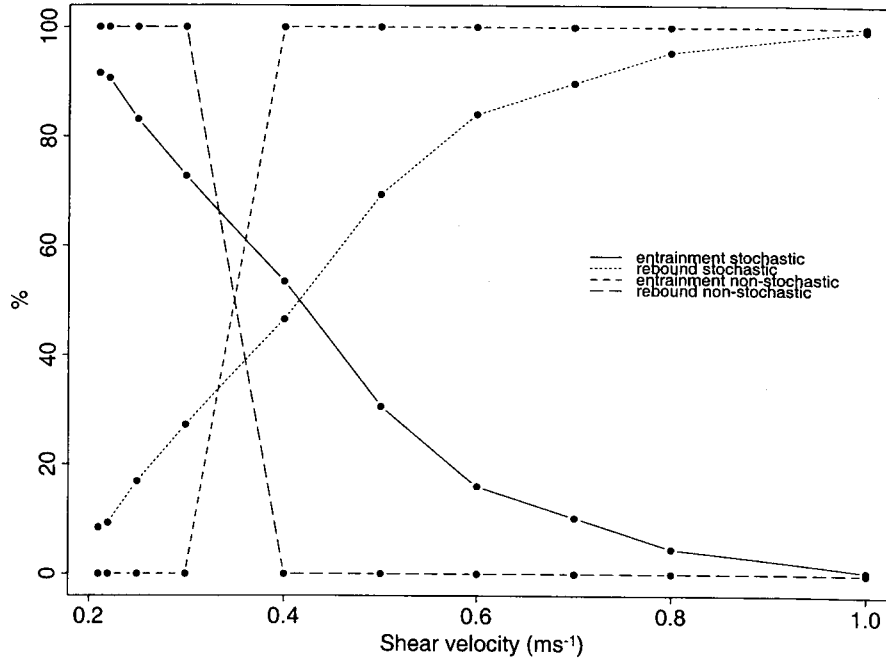
Figure 6. The percentage of aerodynamically entrained and rebounding particles in saltation, as a function of the shear velocity, for both the non-stochastic and the stochastic model. Model parameter values: $d = 0.00048$ m, $\alpha_{ej} = 25°$.

blowing snow. Due to the steady state assumption, some significant simplifications can be made compared to the numerical models developed so far. Nevertheless a good agreement between measured and computed mass fluxes is obtained, which may be an indication that the proposed approximations are justified.

The modification of the shear stress during saltation, and the potential importance of aerodynamic entrainment in this process, are still controversial subjects. A new aspect of the presented model is the fact that the fluid shear stress at the surface is explicitly calculated, based on Owen's hypothesis that it must be at the lowest possible value that ensures mobility of the surface grains. It appears, however, that this value is not fixed, and is dependent on the total shear stress, the elasticity of the particles, and (related to that) the dominant mechanism of particle movement. Furthermore, our theoretical considerations, as well as the results of the numerical simulations, indicate that aerodynamic entrainment may play a larger role during steady state saltation than generally assumed so far. Whereas the conventional assumption is that aerodynamic entrainment is negligible, or at most has a very small contribution, our results state that entrainment can under certain circumstances be the dominant process in saltation.

The presented model is in principle easily adjustable to different granular materials, since the model input parameters are mainly determined by the material
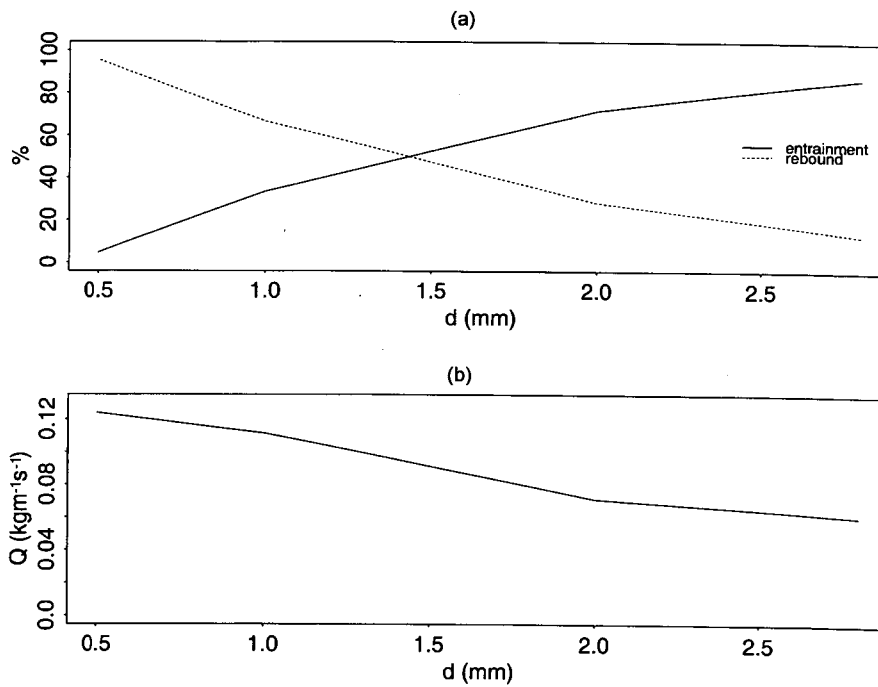
(a)

(b)

Figure 7. Input parameters: $u_* = 0.8$ m s^{-1}, $d = 0.0028$ m, $\alpha_{ej} = 21°$, $r = 0.59$. (a) The percentage of aerodynamically entrained and rebounding particles in saltation, as a function of the grain size; (b) the mass flux as a function of the grain size, keeping all other parameters constant.

properties. In particular for snow saltation this is an important issue, since snow properties are known to change significantly in time. The model parameter that is the most uncertain in our formulations is the aerodynamic entrainment coefficient η_{ae} appearing in Equation (3). In Equation (8) it is made dependent upon only the grain size; it may however well be the case that in reality it is also dependent on grain shape and density. A better estimate of this coefficient could in the future be achieved from measurements of aerodynamic entrainment rates in a wind tunnel.

Another point for future research on saltation will involve the experimental verification of our mass flux formulations in outdoor terrain and atmospheric turbulence. So far the most accurate way of measuring saltating mass fluxes in the field may still be by use of mechanical traps. A complicating factor for this type of measurements is that it is very difficult to distinguish between the saltation layer and the suspension layer. An even more important problem may be the measurement of the shear stress, which is needed as an input parameter for the saltation model. For determining the Reynolds shear stress in atmospheric turbulence, three-dimensional wind data need to be averaged over 20 minutes to one hour. Intuitively, it seems however unlikely that this large time scale is decisive for the snow transport, considering that the saltation process takes place in bursts and waves. It may be therefore that short-term shear stress fluctuations need to be considered when

simulating saltation in the atmospheric boundary layer. This problem requires further investigation of the time scales that are dominant for saltation in nature, and the response time of saltation to a change in wind conditions.

The saltation formulation is developed for use in a complete model of air flow and snow transport in complex terrain, for the purpose of calculating snow distribution patterns. The final goal is to use such a model on an operational basis, for the benefit of avalanche warning. The computational facility of the model is therefore an important benefit, since simulations need to be performed over a large area and in high spatial resolution. The equilibrium assumption for saltation is consistent with the currently existing numerical models of air flow, which are based on Reynolds averaging, and a parameterisation of higher order turbulence terms. In the long term future, it may become possible to use more accurate simulation methods for such a coupled model, such as large eddy simulations or direct numerical simulations. If these methods come within reach, a saltation description comparable to the formulations of e.g., McEwan and Willetts (1991), Anderson and Haff (1991) and Nishimura and Hunt (2000) would be more appropriate. It is, however, highly improbable that this will be an option in the near future. On the other hand, Reynolds averaged numerical simulations of flows have shown their capability, even for very complex situations in fluid mechanics. Therefore, our saltation model is expected to be useful in a coupled air flow – snow drift model. Preliminary results of such computations have been presented in Lehning et al. (2000).

Acknowledgements

References

Anderson, R. S. and Haff, P. K.: 1991, 'Wind Modification and Bed Response during Saltation of Sand in Air', *Acta Mechanica* (Suppl.) **1**, 21–51.

Anderson, R. S. and Hallet, B.: 1986, 'Sediment Transport by the Wind: Toward a General Model', *Geol. Soc. Amer. Bull.* **97**, 523–535.

Bagnold, R. A.: 1941, *The Physics of Blown Sand and Desert Dunes*, Chapman and Hall, 265 pp.

Bintanja, R.: 2000, 'Snowdrift Suspension and Atmospheric Turbulence. Part 1: Theoretical Background and Model Description', *Boundary-Layer Meteorol.* **95**, 343–368.

Gauer, P.: 1999, 'Blowing and Drifting Snow in Alpine Terrain: A Physically-Based Numerical Model and Related Field Measurements', Ph.D. Dissertation, ETH Zürich, Switzerland, 128 pp.

Hunt, J. C. R. and Nalpanis, P.: 1985, 'Saltating and Suspended Particles over Flat and Sloping Surfaces. I. Modelling Concepts', in O. E. Barndorff-Nielsen, J. T. Møller, K. Rømer Rasmussen, and B. B. Willetts (eds.), *Proceedings of the International Workshop of Physics of Blown Sand, Memoirs 8*, Department of Theoretical Statistics, Aarhus University, Denmark, pp. 9–36.

Lehning, M., Doorschot, J., Raderschall, N., and Bartelt, P.: 2000, 'Combining Snow Drift and SNOWPACK Model to Estimate Snow Loading in Avalanche Slopes', in E. Hjorth-Hansen, I. Holand, S. Loset, and H. Norem (eds.), *Snow Engineering*, Balkema, pp. 113-122.

McEwan, I. K.: 1993, 'Bagnold's Kink: A Physical Feature of a Wind Velocity Profile Modified by Blown Sand?', *Earth Surface Proces. Landforms* **18**, 145–156.

McEwan, I. K. and Willets, B. B.: 1991, 'Numerical Model of the Saltation Cloud', *Acta Mechanica* (Suppl.) **1**, 53–66.

Naaim, M., Naaim-Bouvet, F., and Martinez, H.: 1998, 'Numerical Simulation of Drifting Snow: Erosion and Deposition Models', *Ann. Glaciol.* **26**, 191–196.

Nalpanis, P., Hunt, J. C. R., and Barrett, C. F.: 1993, 'Saltating Particles over Flat Beds', *J. Fluid Mech.* **251**, 661–685.

Nishimura, K. and Hunt, J. C. R.: 2000, 'Saltation and Incipient Suspension above a Flat Particle Bed below a Turbulent Boundary Layer', *J. Fluid. Mech.* **417**, 77–102.

Nishimura, K., Sugiura, K., Nemoto, M., and Maeno, N.: 2000, 'Measurements and Numerical Simulations of Snow-Particle Saltation', *Ann. Glaciol.* **26**, 184–190.

Owen, P. R.: 1964, 'Saltation of Uniform Grains in Air', *J. Fluid. Mech.* **20**, 225–242.

Pomeroy, J. W. and Gray, D. M.: 1990, 'Saltation of Snow', *Water Resour. Res.* **26**, 1583–1594.

Raupach, M. R.: 1991, 'Saltation Layers, Vegetation Canopies and Roughness Lenghts', *Acta Mechanica* (Suppl.) **1**, 83–96.

Shao, Y. and Li, A.: 1999, 'Numerical Modelling of Saltation in the Atmospheric Surface Layer', *Boundary-Layer Meteorol.* **91**, 199–225.

Sørensen, M.: 1991, 'An Analytic Model of Wind-Blown Sand Transport', *Acta Mechanica* (Suppl.) **1**, 67–81.

Stull, R. B.: 1988, *An Introduction to Boundary Layer Meteorology*, Kluwer Academic Publishers, Dordrecht, 666 pp.

Willetts, B. B. and Rice, M. A.: 1989, 'Collision of Quartz Grains with a Sand Bed: The Influence of Incident Angle', *Earth Surface Proces. Landforms* **14**, 719–730.